Engineering Structures 210 (2020) 110413

Contents lists available at ScienceDirect

Engineering Structures

journal homepage: www.elsevier.com/locate/engstruct

Ultrasonic inline inspection of a cement-based drinking water pipeline

Hector Hernandez Delgadillo[a,b,*], Caspar Geelen[b,c], Rutger Kakes[b,d], Richard Loendersloot[a], Doekle Yntema[b], Tiedo Tinga[a], Remko Akkerman[a]

[a] Faculty of Engineering Technology (ET), University of Twente, Drienerlolaan 5, 7522 NB Enschede, The Netherlands
[b] Smart Water Grids Theme, Wetsus European Centre of Excellence for Sustainable Water Technology, Oostergoweg 9, 8911 MA Leeuwarden, The Netherlands
[c] Biometrics, Wageningen University, Droevendaalsesteeg 4, 6708 PB Wageningen, The Netherlands
[d] Biobased Chemistry and Technology, Wageningen University, Droevendaalsesteeg 4, 6708 PB Wageningen, The Netherlands

ARTICLE INFO

Keywords:
Cement-based pipeline
Inline inspection
Data processing
Degradation

ABSTRACT

The integrity of the drinking water infrastructure deteriorates with time. Monitoring the condition of the drinking water mains can enhance the remaining operational lifetime assessment of the network. In this research a method to translate ultrasonic signals to degradation levels from an inline inspection in a cement-based drinking water pipeline is proposed. The data was obtained from an inspection performed in a Dutch drinking main section. The data is processed in two major steps. Firstly, the parameters that provide the condition of the cement are extracted. Secondly, images of the degradation within the pipes of the inspected trajectory were generated. The main contributions in this paper are (i) the estimation of relative degradation levels of a cement-based pipeline based on the ultrasonic pulse-echo technique and (ii) the upscaling of the processing method in an automated manner for visualization of the degraded condition. Lastly, a sensitivity study of the parameters relevant to the determination of the degraded depth has been performed. The speed of sound in cement is the most relevant parameter to consider. Estimating absolute degradation levels needs further study.

1. Introduction

Preventing failure of drinking water distribution systems is a current interest in many countries around the world. Repairing a failed pipe can cost tens of thousands of Euros. What is more, interruption of the supplied water and third-party damages are further consequences of a failed pipe. This raises the question of how to prevent failure in the drinking water network. The replacement of the mains can be performed effectively if the state of the pipe is known. In this research, a methodology that can detect and determine the degraded thickness in a cementitious structure is applied to a real cement-based drinking water pipe.

Cementitious pipes account for nearly 30% of the Dutch drinking water network [1]. In today's condition assessment market, there are two types of non-destructive inspection methods that have been used to determine the degradation levels in cement-based pipes. These are acoustic-based techniques and surface penetrating radar (SPR) [2–9]. The acoustic-based technique monitors the travel time of an acoustic wave, generated from tapping an accessory within the network (e.g. a nearby valve), at least at two different locations along the pipeline, with acoustic sensors. These sensors have to be in direct contact with the surface of the pipeline or in direct contact with the other type of accessories. By measuring the speed of the propagating sound wave, the average condition of the material can be determined [5,7,9]. Another derivation of this technique is known as the hydraulic transient analysis (HTA), where major advancements have been made in wave propagation modelling for prediction of deterioration, sensor placement optimization, advanced signal processing algorithms and the use of different acoustic sources [10–14]. These acoustic-based technologies are focused on a continuous monitoring of the wave speeds. The main disadvantages are the complex extraction of the relevant parameters, complex signal processing algorithms and the required adequate sensor placement. Furthermore, it only gives the average condition of the monitored length.

The SPR method consists of transmitting radio waves from the outer surface of the pipe. These radio waves are transmitted/reflected at the boundary between different material properties and are recorded with an acquisition unit. The local through-thickness degradation level is contained in the reflected waves [2,4]. The main disadvantages of the SPR technique are that the pipes must be dug out, which is costly and time-consuming, the inspection technique is dependent on the technician skills and the condition assessment is local, hence not representative for the entire pipe segment and even limited to the size of the sensor. None of these major techniques is sufficiently versatile to be used in a routine

* Corresponding author at: Faculty of Engineering Technology (ET), University of Twente, Drienerlolaan 5, 7522 NB Enschede, The Netherlands.
E-mail address: h.hernandezdelgadillo@outlook.com (H. Hernandez Delgadillo).

https://doi.org/10.1016/j.engstruct.2020.110413
Received 1 August 2019; Received in revised form 15 January 2020; Accepted 20 February 2020

fashion nor provides detailed information on the complete pipe section.

Another type of condition assessment in cement-based pipes is the detection of leaks. Leaks are detected most commonly with acoustic-based techniques (hydrophones) and pressure-based sensor data [15–18]. Other techniques that have been subject of research are based on the use of optical sensors, placement of wireless sensors within the network and vibration-based measurements, amongst others [18–22]. Most of these techniques seem promising, however, fundamentally the water loss from a cracked pipe is due to material deterioration. In this research, the main goal is to measure the condition of a drinking water pipeline before the crack initiates and in turn potentially reduce maintenance costs and operational downtimes.

Naffa et al. [23] demonstrated that by measuring the speed of sound in concrete, it is possible to detect chemical damage, however, estimating the damage level remained a matter of research. In a different study, Demĉenko et al. [24] showed that, based on the reflection from the deteriorated layer, it is possible to detect and measure the remaining healthy thickness of a cement degraded by acid. This approach is very effective when the acoustic impedance between the degraded material and healthy material is relatively high. In a more recent study, a methodology to quantify through-thickness chemical degradation in cementitious structures based on high frequency sound waves was developed [25]. Estimating the degradation level is done by measuring the acoustic pulse velocity through the thickness of the material. A major challenge in the latter technique is that the pipe's thickness and speed of sound in pristine and fully degraded conditions have to be known [25,26].

In collaboration with Acquaint B.V., an inspection company, the inspection data from an inspected section from the Dutch drinking water grid is used. The first objective of this research is to determine the degradation levels in the inspected pipeline [25], based on the pulse-velocity methodology. The second objective is to provide a processing method that enables upscaling of the parameter extraction and visualization of the estimated degraded depth. Finally, the sensitivity of the parameters that can influence the estimation of the degraded depth is investigated.

2. Estimation of degraded depth in a cementitious structure

In a deteriorated cementitious structure, it is possible to determine the thickness of the degraded layer based on the time-of-flight of the acoustic waves. The degradation of cement-based structures generates a difference in material properties from the external surfaces towards the inside of the material. Extensive information on chemical deterioration of cementitious structures is available in literature stating that the most relevant degradation mechanism for drinking water pipelines is calcium leaching [8,27–34]. When a cement structure is in contact with an aggressive environment (low pH medium or low ion content water), calcium starts to leach out from the surface of the cement [31,32]. Calcium leaching reduces the strength of the structure [30]. Fig. 1a and 1b depict the layers that are generated due to calcium leaching. The degraded zone is shown as d in both figures, h is the healthy zone and D is the total wall thickness. Fig. 1a depicts degradation from one side only and Fig. 1b depicts degradation from the two sides (inner and outer pipe surface) of the structure. Both cases should be present in a cement-based water pipeline, nonetheless, the two-sided degradation is more likely to occur due to the contact with soil and the conveyed water [25].

The time that an acoustic wave takes to travel from the top surface to the bottom surface (see Fig. 1a and 1b) is the sum of the time it takes in the degraded region and in the healthy region:

$$t_D = t_h + t_d \tag{1}$$

where $t_d = t_{di} + t_{do}$, for the two-sided degradation case. For each region of the specimen, the distance over velocity is substituted:

$$t_D = \frac{2h}{V_h} + \frac{2d}{V_{fd}} \tag{2}$$

where $d = d_o + d_i$ for two-sided degradation, the subscript fd refers to the speed of sound in fully degraded material and V_h is the speed of sound in pristine cement. It is important to distinguish between degraded and fully degraded [25]. The term degraded refers to a cement material that contains both a fully degraded and a healthy part. Fully degraded refers to only the part of the specimen that is completely (fully) degraded. The remaining healthy component is defined as

$$h = D - d \tag{3}$$

where D is the thickness of the specimen. The fully degraded speed of sound is defined as a fraction of the speed of sound in healthy material

$$V_{fd} = \gamma V_h \tag{4}$$

where γ is the ratio of fully degraded speed of sound and healthy speed of sound and was found to be 0.54 in an earlier research [25]. By substituting Eq. (3) and Eq. (4) in Eq. (2), the thickness of the degraded layer is

$$d = \frac{0.5 t_D V_h - D}{\gamma^{-1} - 1} \tag{5}$$

The time t_D is extracted from the ultrasonic data as Δt. The degraded depth can be determined if the speed of sound in pristine and fully degraded condition are known. It is expected that for a field pipe test, both quantities will be unknown and nearly unattainable, thus, in this work these two quantities are assumed based on literature [25].

3. Methodology

This section is divided in three main parts. In the first part, details on the performed inspection, including the trajectory and specifications of the inspection tool, will be given. Then, the principle of the ultrasonic tests together with the processing of the signals from ultrasonic raw responses to time-of-flight information is discussed. The third part, the visualization section, focuses on handling the extracted parameters such that the degraded state can be understood qualitatively and quantitatively.

3.1. Inspection tool and inspected trajectory

A cement-based pipeline was inspected with an inspection tool equipped with eight ultrasonic sensors. The tool is made of a cylindrical foam (black colour in Fig. 2) that is compressible to the inner diameter of the pipe. It is equipped with eight ultrasonic transducers as depicted

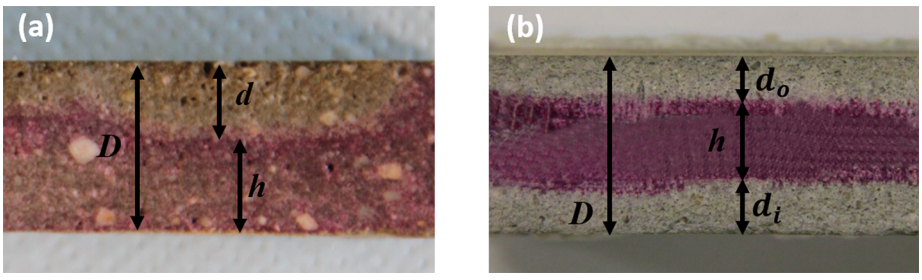

Fig. 1. Leached cementitious structure treated with phenolphthalein to determine the pH value. The colourless region (d) represents the degraded material (low pH) and the purple region represents non-degraded material (pH still high enough). (a) one-sided degradation and (b) two-sided degradation.

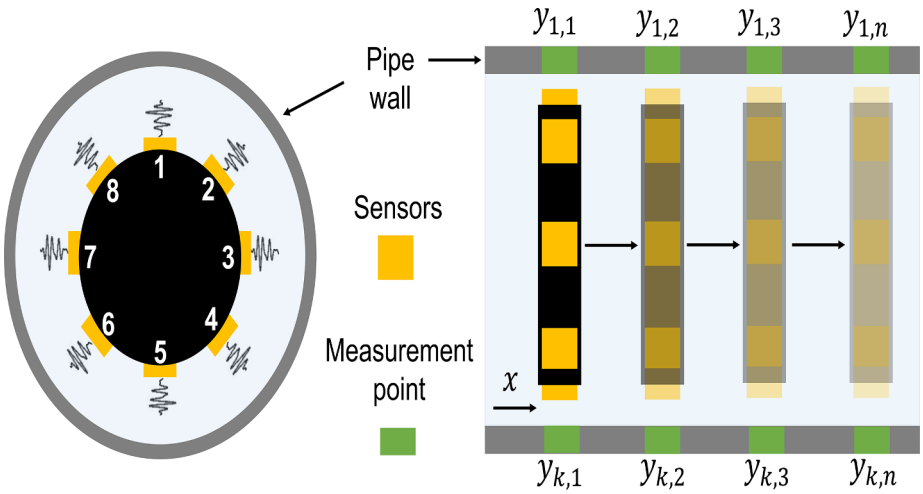

Fig. 2. Schematic representation of the inspection tool in a pipe section, with front view (left) and side view (right). The tool carries 8 ultrasonic transducers along the circumference. Each sensor transmits acoustic waves through the water, that further propagates through the thickness of the pipe, and reflects back to the transducer resulting in measurements at locations $y_{k,n}$.

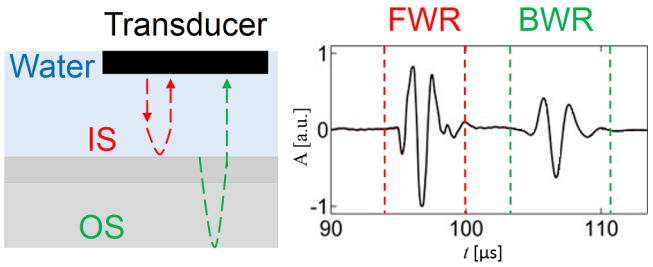

Fig. 3. Reflection of sound waves at the inner surface (IS) and outer surface (OS) of the pipe from the front-wall reflection (FWR) and from the back-wall reflection (BWR) respectively.

in Fig. 2. Each sensor performs a measurement every 0.05 s. The tool translates through the pipe at a speed of approximately $c = 0.2$ m/s. The tool is tracked above ground which allows the accurate correlation between the acoustic measurements and the location along the pipeline. Rotation of the inspection tool is corrected with rotational sensors embedded in the inspection tool. The inspection system acquires 160 measurements per second and approximately 800 measurements per meter of inspected water main trajectory.

The face of the ultrasonic transducers is aligned parallel to the internal surface of the pipe (see Fig. 2). Each transducer is excited by an electric pulse which in turns converts electrical energy into mechanical energy (acoustic waves). These waves travel through the water (as shown in Fig. 2). The transition from water-to-inner-surface and outside-surface-to-soil interfaces produce energy transmission and reflection (see Fig. 3). The energy that is reflected at the water-to-inner-surface interface is called the front wall reflection (see Fig. 3). The transmitted acoustic waves then travel through the thickness of the specimen. At the outside-surface-to-soil interface, most of the energy is reflected and some energy is transmitted to the surrounding soil. The energy that is reflected at the latter interface is called the back-wall reflection (see Fig. 3). The front wall and back wall reflections are the main waves of interest that are recorded by the ultrasonic transducer.

The inspection was done in 2018 and its geographical location is shown in Fig. 4 (green line). The inspected trajectory length is 1939 m. The tool has a location tracker, such that the inspected trajectory can be visualized on a map as shown in Fig. 4.

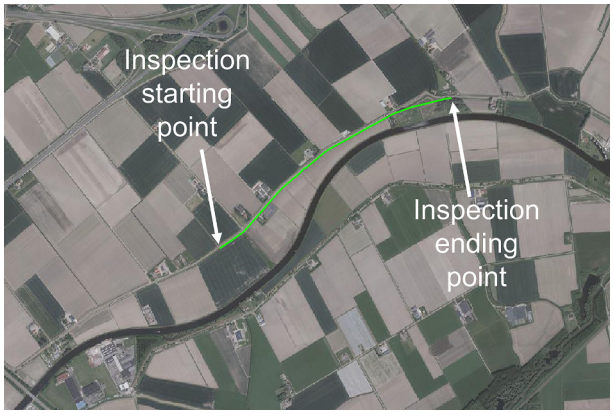

Fig. 4. Aerial view of inspected pipeline section.

3.2. Automatic processing of ultrasonic signals

The objective of data processing is to translate the obtained raw ultrasonic signals to a parameter related to the amount of degradation. This is achieved by estimating the time difference Δt between front and back wall time-of-arrival (see Fig. 3). The processing of the acquired data is performed with the same scheme as presented in [25,26].

With the vast amount of data being processed, automation is necessary. The front wall and back wall reflections are automatically detected with the following process. First, the absolute magnitude of the derivative of the entire recorded signal is calculated (see Fig. 5b). Then, the maximum value of the data set is located (black point in Fig. 5b). Based on the present pipe thickness, acquisition rate and central frequency of the sensor, 6% of the total signal length is selected (vertical black lines in Fig. 5a) avoiding overlapping with other nearby reflections. This accounts for approximately 6.5 μs of time delay (x axis in Fig. 5). The signal within the selected 6% is replaced by zero values to create a convenient sample size, as shown by the horizontal line in Fig. 5b. The replacement of the front-wall by zero values enables the detection of the back-wall maximum peak without modifying the length of the data set. Thereafter, the derivative of the original signal, plus the section replaced by zero values, is calculated and a second maximum is located (red point in Fig. 5b). Similarly, the back-wall reflection contained in 6% of the total signal is extracted. At this stage, two signals have been extracted: front-wall and back-wall reflections both with 6% ($\approx$6.5 μm) of the total data length.

The main advantage of this procedure is that the maximum amplitude of the front-wall and back-wall reflections are located in an automatized manner. Reflections from the internal layer are present only in a limited part of the data and are lower in amplitude than the front-wall and back-wall. As described in [25], reflections from the internal layer (due to calcium leaching) in a cement-based structure are present only if the difference in acoustic impedance between the healthy and the degraded region is relatively large. The presence of such reflection in part of the inspection data means that the degradation is not

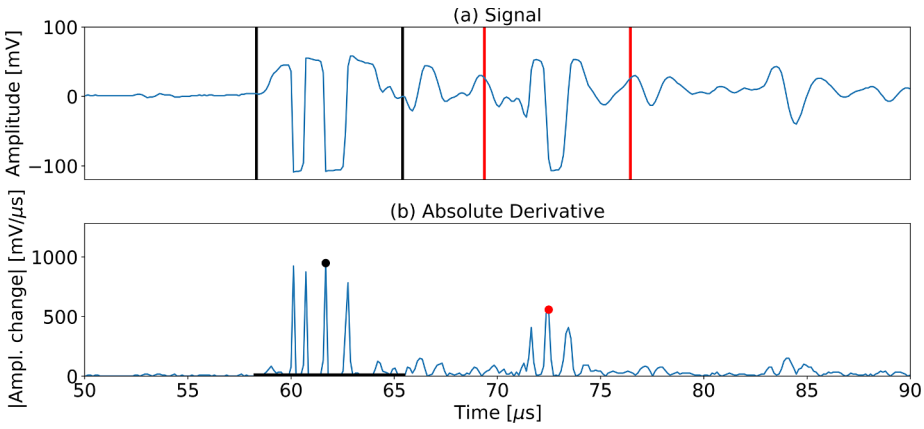

Fig. 5. Signal processing scheme. (a) Time signal with the selected limits for the extraction of the front wall (black lines) and back wall (red lines); (b) Absolute derivative with the section replaced by zero values (bottom black line) and the maximum amplitude of front wall (black point) and maximum amplitude of back wall (red point).

homogeneous throughout the pipeline. In general, ultrasonic pulse-echo cannot rely on such reflection for monitoring the condition of cement-based drinking water pipelines.

To further process the selected reflections (front wall and back wall) a band-pass filter is used. An example of the band-pass filter scheme and process is described in [25,26]. Finally, the difference between the time-of-arrival of the FW and BW signals () is calculated and Eq. (5) is then solved. The following assumptions are made in this analysis: (i) throughout the trajectory the wall thickness is constant; (ii) degradation is mostly a general process, thus local changes are not expected; (iii) and degradation is homogeneous along the pipe circumference.

3.3. Visualization of extracted parameters

Large variations on the measurements are expected and can arise due to several reasons: the joints between pipes, tool wobbling (resulting in low amplitude reflections), low signal-to-noise ratio and inadequate signal filtering. These faulty and noisy signals are removed. Thereafter, a moving average filter was used on the calculated time-of-flight difference (Δt) of each sensor separately. Assuming a uniform degradation along the pipe circumference, the data from all eight sensors was averaged. For each measurement location, three values were extracted: the maximum, the minimum and the average of the time difference Δt. Finally, the degraded depth was calculated from Eq. (5). One advantage of averaging the 8 sensors is that, severe damage can be detected immediately and it is corroborated with the maximum and minimum, if these quantities increase. On the contrary, if local degradation is present along the circumference, the averaging method will not detect these, however, the maximum and minimum can trigger a more detail observation on these areas.

The data processing is shown in Fig. 6. In the top figure three different lines of data are shown (i) the light blue line depicts the time difference Δt for one sensor without processing, (ii) the dark blue line depicts the time difference Δt after application of a moving average for one sensor and (iii) the red line represents the average of the eight sensors, again after application of moving average to each of them. The colour map in the lower part of Fig. 6 shows the time difference Δt for each individual sensor. The blue vertical lines in the figure on the top represent the joints between pipe sections (the joints are in between two closely spaced lines). The x axis for both parts of the figure represents the distance along the inspected trajectory.

The time difference indicated by the red line (average over 8 sensors) is slightly higher in comparison with the time difference indicated by the dark blue line (single sensor) from 1365 m to 1368 m (see Fig. 6). On the contrary, single sensor time difference is slightly higher than the averaged sensor time difference from 1378 m to 1382 m (see Fig. 6). This effect is due to the averaging over the eight sensors. For both cases, the colour map reflects the real time difference at a particular location for a particular sensor. Thus, the averaged sensor time difference in the top figure (the averaging method) serves as a guide for detecting major changes in degradation along the longitudinal direction of the inspected trajectory.

The degraded depth is then estimated based on Eq. (5), assuming a constant total wall thickness. With the processing scheme presented in this research, the ultrasonic data can be visualized in a way that provides the optimal information to evaluate the condition of the cement-based pipeline. The calculated degraded depth will be shown in an aerial view of the trajectory (averaging method), similar to the one in Fig. 4. This facilitates the localization of areas that appear to have higher degradation. The degradation patterns within this type of pipelines are unknown, therefore, the data from the 8 sensors will be examined as well.

4. Results and discussion

4.1. Sensor parameters

A boxplot depicting the time-of-flight difference Δt per sensor over the complete inspected trajectory from the filtered data is shown in

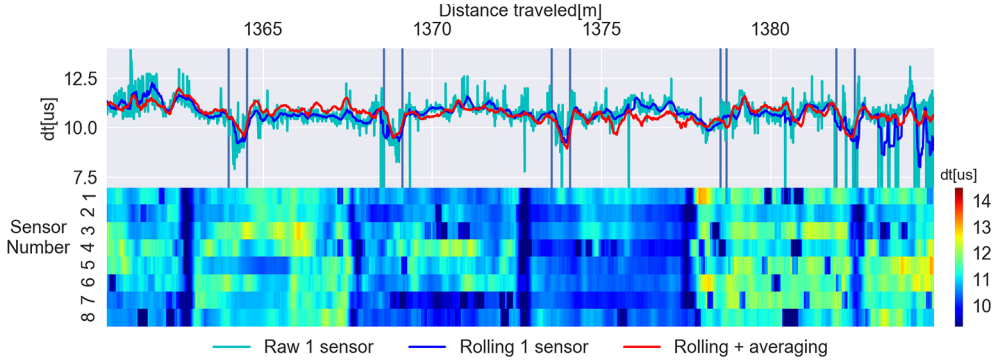

Fig. 6. Visualization of time of flight differences along a pipe section. Single sensor (nr.5) data (raw and moving average) and averaged data are shown as lines in the top part, and the color map in the lower part shows the Δt moving average per sensor.

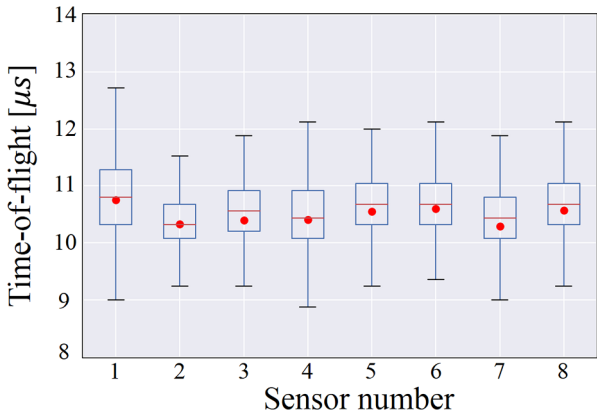

Fig. 7. Boxplot of the time of flight variation over the inspected trajectory with the median (red line) and average (red dot) values per sensor. The black lines represent the 75% quartiles and the boxes represent the 25% quartiles.

Fig. 7. The mean and median values are very similar in all sensors, which indicates a normal distribution of the degradation along the pipe circumference. This permits the use of the averaging method only for degradation along the longitudinal direction. Larger deviation between sensors statistics would not enable the use of the averaging method. Two major reasons are a malfunctioning sensor and significant difference in degradation patterns mainly along the pipe circumference. For the first case, the data from a faulty sensor could be removed. For the second case, the averaging method could hinder the detection of degradation. The data from the eight sensors were analysed in order to characterize difference in degradation levels along the circumference.

The use of the data distribution describes if there is high deviation between the individual sensor values. Based on this, it possible to determine if a sensor is working properly or if the sensors are measuring completely different quantities (e.g. degradation levels). The statistics tell that it is possible to do an averaging, as the variation across the sensors is rather limited.

4.2. Results of inspected section

The average degradation depth per measurement location was used to generate one quantitative degradation depth variation over the inspected trajectory. This is an estimate of the amount of leaching in the pipe at that specific measured point. The leaching depth is estimated assuming a constant pipe wall thickness. The degraded depth values are shown for segments of 100 m. Assuming a fairly homogeneous acoustic velocity in its pristine state, the degraded depth can only be attributed to chemical degradation. However, throughout the trajectory, certain pipe sections show a behaviour that is inconsistent with these assumptions. Four examples of these inconsistent events are discussed to describe the phenomena responsible for aberrant degraded depth measurements.

(I) Sudden degraded depth change between neighbouring pipes

In Fig. 8 at 455 m, a sudden increase in degradation depth between to the left and right neighbouring pipe sections can be seen. If the assumption that the thickness is constant throughout the inspected trajectory is true, it would mean that a 6 mm degradation difference exists between the pipe at 455 m and the two pipes next to it. The opposite behaviour can be seen at 460 m (the pipe contiguous to the one with the highest degraded depth).

The significant and abrupt changes in degradation depth in these locations can be explained in three ways. Firstly, considering the assumption that the pipe wall thickness is constant, the pipe with the higher degradation would have to be buried in soil or convey water that is more aggressive than at its neighbours on the right and on the left. Thus, it would be a very special case were only that specific pipe has severe damage. Another reason why this could happen, and still considering the assumption that the thickness is constant, is that the pipe with the lowest degradation has already been replaced before, and thus is actually "healthier". For the case at 460 m (low degraded depth), the latter seems realistic as there is only one pipe section that has low degradation depth. However, for the case at location 455 m, the outlier is the pipe section with the highest degraded depth. A third possibility is that the assumption of constant pipe thickness is incorrect for those specific pipe sections. However, since no data on actual pipe thickness, or the thickness standard deviation as a result of the production process, is available, assuming a constant pipe thickness is the best option, especially considering that this assumption seems to hold for most pipe sections.

(II) Gradual increase/decrease of degraded depth in a pipe section

In Fig. 9 at around 955 m and 985 m a considerable increase in degradation depth along one pipe section is observed. This would mean that the degradation progressively increases from the beginning of a single pipe segment towards the end. The difference between the highest and lowest degraded points is 7.34 mm. This same behaviour is seen at 410 m in Fig. 8. A possible explanation would be a variable wall thickness.

(III) Consistent degradation along the longitudinal direction

A third relevant behaviour that is observed throughout the inspected trajectory as a trajectory-wide behaviour. This effect can be better seen in Fig. 10. The trend within each pipe section is not isolated (as in the previous examples) but it is consistent with the neighbouring pipe sections. For instance, from 1200 m to 1400 m in Fig. 10 a higher

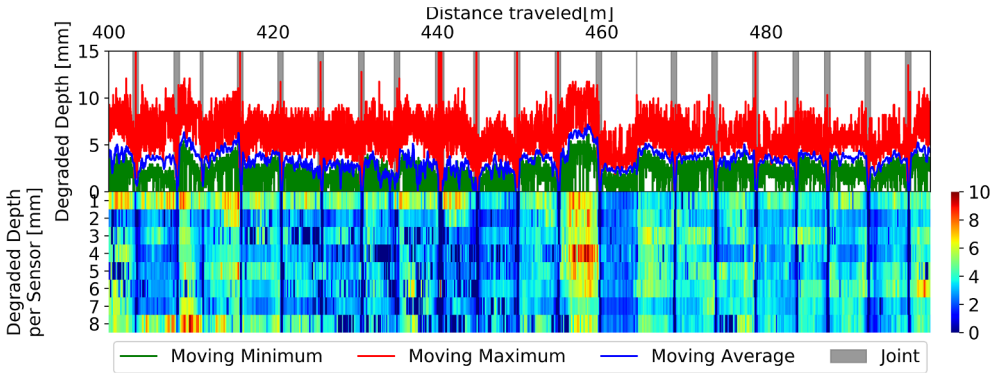

Fig. 8. Estimated degraded depth distribution for section from 400 to 500 m. The solid line in blue represents the averaged data for the eight sensors; the line in red represents the maximum and the line in green represents the minimum values. The colour maps show detected degraded depth at each individual sensor.

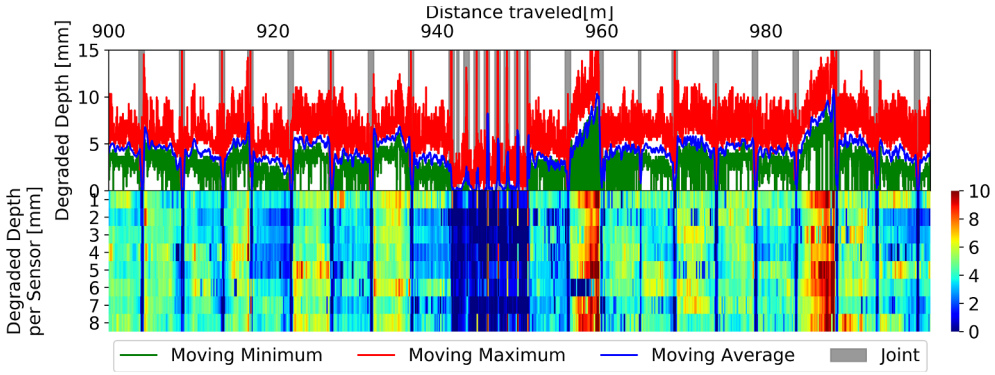

Fig. 9. Estimated degradation depth distribution for section from 900 to 1000 m. The solid line in blue represents the averaged data for the eight sensors; the line in red represents the maximum and the line in green represents the minimum values. The colour maps show degraded depth for each individual sensor.

degradation depth is seen compared to adjacent sections (from 1010 m to 1200 m and from 1400 to 1600 m). This accounts for at least 200 m of the inspected trajectory. Furthermore, the degradation depth changes gradually rather than sharply. A similar, but more localized, pattern can be seen in Fig. 10, approximately at 50 m, 250 m, 750 m and 1000 m. In these sections, there is high degradation depth compared to adjacent sections. Leaching of calcium is expected to occur more globally than locally, as it is caused by the surrounding environment, especially the soil. Thus, calcium leaching would be expected to be present more often in several adjacent pipes than in one pipe only.

In Fig. 10, the outliers found by the average per pipe and by the maximum per pipe are related to change in pipe material. An example of this can be better seen in Fig. 9 in the travelled distance between 940 m and 950 m where the apparent degradation depth drops to zero. In that section of the network a different type of pipe was installed. Similarly, in the distances at approximately at 750 m, 1500 m and 1770 m, other types of pipes are detected (see Fig. 10).

(IV) Apparent difference in degradation along the circumference

The fourth and last observed behaviour in the inspected trajectory is the apparent difference in degraded depth along the circumference of the pipe. Considering the assumed homogeneity in pipe wall thickness throughout the inspected trajectory, this would mean that degradation differs along the circumference in cement-based pipes. This effect is depicted in Fig. 11 at 1660 m, 1610 m and 1645 m, where half of the sensors detect a higher degradation depth than the other half of the sensors. This behaviour is observed as well in Fig. 9 at 920 m.

The detection of circumferential degradation is hindered by the use of averaged values. Thus, the averaging method is used only to get an overview of the degradation along the pipeline longitudinal direction. The data analysis should be performed for the eight sensors separately. It is recommended to further investigate the possibility to use more advanced signal processing schemes (e.g. machine learning) for a robust detection of degradation in both the longitudinal and circumferential directions.

After considering the four main types of deviations, the increase/

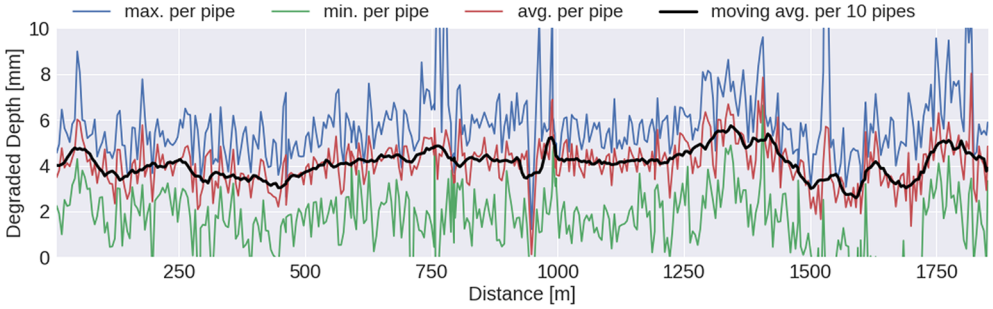

Fig. 10. Estimated degradation depth distribution for the entire inspected trajectory. The data shown is extracted from the eight sensors for each individual pipe. The line in blue represents the maximum degraded depth; the line in red represents the average degraded depth and the line in green represents the minimum degraded depth. The line in black represents a moving average filter per 10 pipe sections.

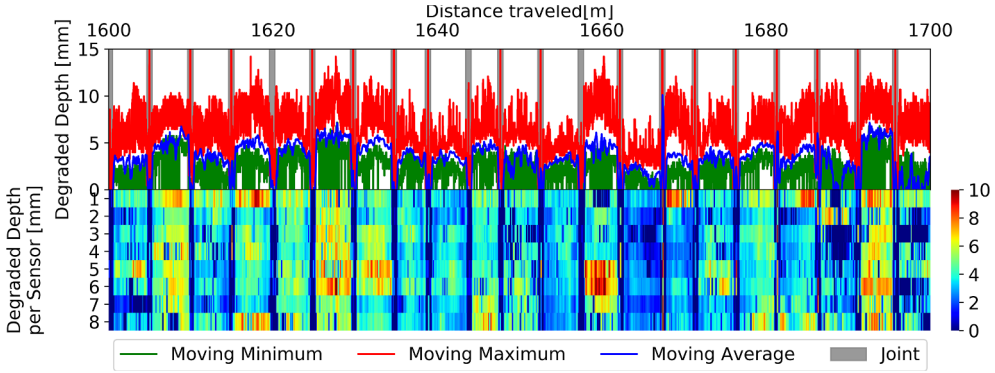

Fig. 11. Estimated degradation depth distribution for section from 1600 to 1700 m. The solid line in blue represents the averaged data for the eight sensors; the line in red represents the maximum and the line in green represents the minimum values. The colour maps show degraded depth for each individual sensor.

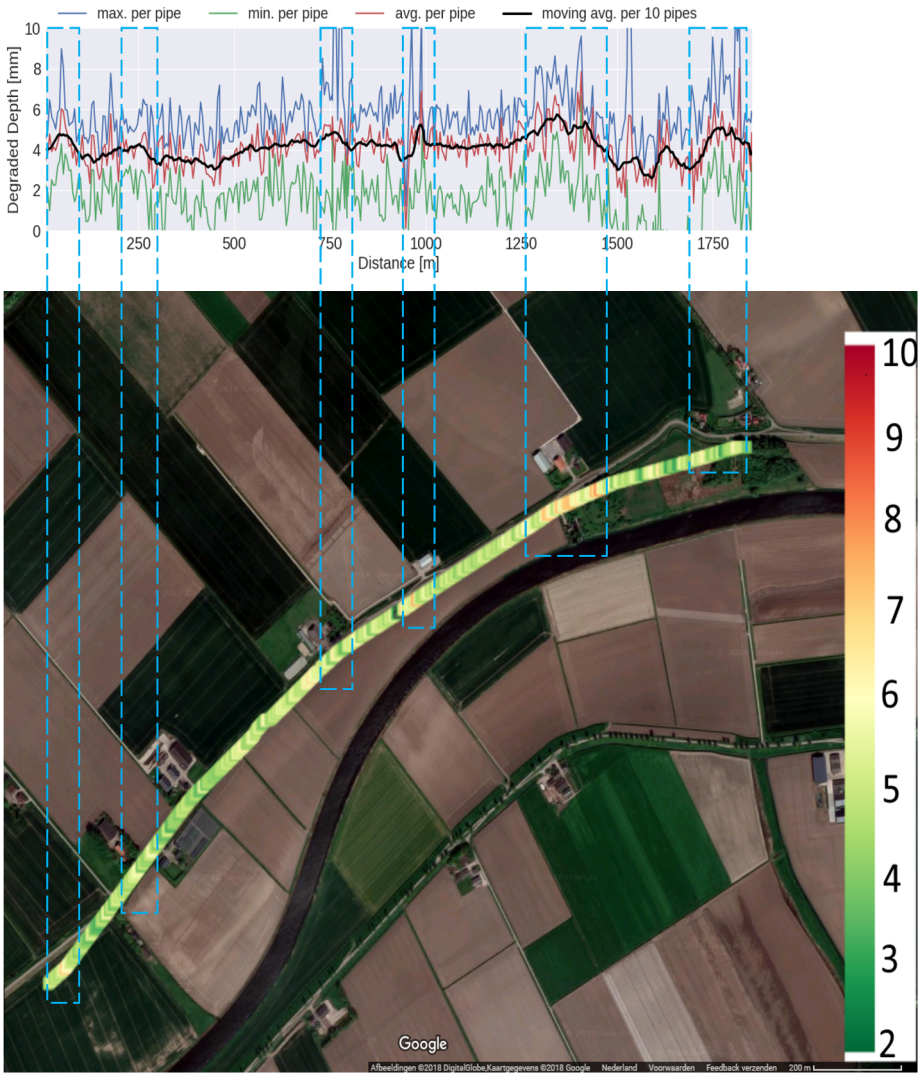

Fig. 12. Aerial view of the estimated degraded depths along the inspected trajectory.

decrease of estimated degraded depth in a single pipe section from start to end is the most remarkable behaviour. The assumption that the thickness is constant is potentially wrong (only for observation *II*) as the absolute leaching depth suggests unrealistic wall thickness reduction or manufacturing imperfections. If this would be the case, the maximum apparent thickness change would be 6.25 mm (for a nominal thickness of 23 mm). This thickness variation accounts for 25% change in thickness. It is likely to be a combination of production flaws and different degradation levels.

In Fig. 12, the calculated degraded depth variation is shown in an aerial view along the inspected trajectory. For this visualization, the average degradation depth from the eight sensors is used to display the degraded depth. However, with this visualization it is not possible to see when there is circumferential degradation. Using the average degraded depth per eight sensors is not valid in cases with circumferential degradation. If the maximum and minimum degradation depths shown in Fig. 11 increase or decrease together with the average degraded depth, then the estimated degraded depth at that location is not an outlier. When the maximum degraded depth increases and the average degraded depth does not change, the estimated degraded depth at that location is considered an outlier. The outliers are due to change in material pipe and due to low amplitude signals.

In correlating the areas with apparent higher degradation with the surrounding environment, an increase in degradation appears to be mostly in areas next to farms. The land usage can thus have a relevant effect on the degradation levels and on the degradation rate for instance a difference in soil pH or moisture. The degradation levels shown from the aerial view in the map is a very useful way to investigate the possible causes of changes in the ultrasonic responses. In this way a better understanding of the possible causes of degradation can lead to improved failure predictions.

4.3. Sensitivity

The parameters that could introduce deviations to the estimated depth are: the implemented filter parameter (f_c), wall thickness, speed of sound in pristine state and speed of sound in fully degraded cement (γ in Eq. (5)). In this section, the sensitivity of each of these parameters is investigated. In Fig. 13, the sensitivity to the estimation of the degraded depth is shown. The used ranges for the various parameters are shown in Table 1.

It is observed that the parameters with the highest sensitivity are the pristine and fully degraded speed of sound in cement, followed by the wall thickness. The filter parameters do not have a strong effect on the estimation of the degraded depth. A 10% deviation in the filter parameter induces only 3–7% error in the estimation of the degraded depth, depending on whether the parameter is increased or decreased.

A 5% change in the speed of sound in pristine condition already

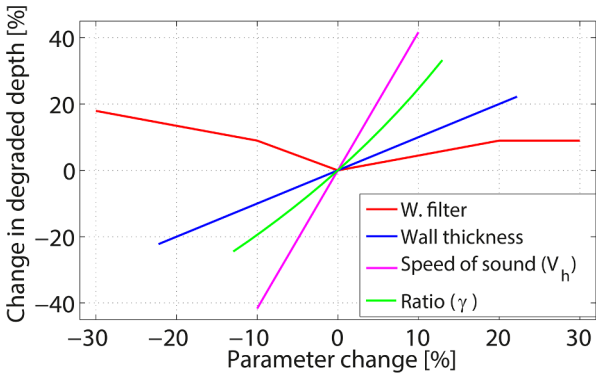

Fig. 13. Sensitivity of the estimated degraded depth for variations in filter coefficient, pipe wall thickness, speed of sound in fully degraded material (γ in Eq. (5)) and speed of sound in pristine condition.

Table 1
Upper and lower limits for the sensitivity analysis.

	f_C	D [mm]	V_h [m/s]	γ
Lower limit	$(0.7 * f_C)$	18	4500	0.47
Upper limit	$(1.3 * f_C)$	28	5500	0.61

induces a 20% error in the estimation of the degraded depth. An error of 5% in the fully degraded speed of sound (γV_h) induces an error of 10% in the calculated degraded depth. Thus, these two parameters are fundamental. A 5% error in the wall thickness would induce a 5% error in the estimated degraded depth. Thus, there is a higher allowable range for errors in the thickness.

Assuming a constant thickness is an effective approach, however, in some isolated cases, this is not valid. The actual thickness of the installed infrastructure is unknown, thus determining the absolute value of the degraded depth remains unattainable. However, differences in apparent degradation depth can be clearly identified with the proposed method. These can then trigger further investigation with other techniques at only these specific locations. This selection of critical locations can already imply huge cost savings compared to a situation in which a complete section must be analysed in detail or even replaced.

Further CT scans have validated the degradation levels along the circumference. The latter results are not yet public and were obtained by Acquaint B.V. in collaboration with KWR water research.

5. Conclusion

In this research, the possibility to inspect and evaluate cement-based pipes with the ultrasonic pulse echo technique was confirmed. Furthermore, the developed method to process the ultrasonic responses can be used for a large amount of measurement data. The colour maps present a powerful tool to identify large changes in degraded depth within pipe sections in the inspected water grid as well as in the circumference of each pipe. The averaging method is useful to localize severe damage along the pipe length and the colour maps are useful to detect severe damage along the circumference. Only relative degradation levels can be estimated. Determining the absolute degradation levels is a matter of further research.

It was found that the two most important parameters that have to be correctly determined are the speed of sound in the pristine condition and in the fully degraded condition.

Along the inspected trajectory, the visualization of the estimated degraded depth showed many interesting sections. Assuming that the pipe wall thickness is constant throughout the whole trajectory seems valid, since firstly the signals from the majority of the inspected trajectory were consistent with those of neighbouring pipes, and secondly since this assumption does not induce large errors in the calculated degraded depth.

CRediT authorship contribution statement

Hector Hernandez Delgadillo: Conceptualization, Methodology, Software, Validation, Formal analysis, Investigation, Resources, Data curation, Writing - original draft, Writing - review & editing, Visualization, Project administration. **Caspar Geelen:** Conceptualization, Methodology, Software, Validation, Formal analysis, Investigation, Resources, Writing - review & editing, Project administration. **Rutger Kakes:** Conceptualization, Software, Validation, Formal analysis, Investigation, Data curation, Visualization. **Richard Loendersloot:** Conceptualization, Formal analysis, Resources, Writing - review & editing, Supervision, Project administration, Funding acquisition. **Doekle Yntema:** Conceptualization, Formal analysis, Resources, Writing - review & editing, Supervision, Project administration, Funding acquisition. **Tiedo Tinga:** Conceptualization, Formal analysis, Resources, Writing - review & editing, Supervision, Project administration, Funding acquisition. **Remko Akkerman:** Resources, Writing - review & editing, Supervision, Project administration, Funding acquisition.

Acknowledgment

This work was performed in the cooperation framework of Wetsus, European Centre of Excellence for Sustainable Water Technology (www.wetsus.eu). Wetsus is co-funded by the Dutch Ministry of Economic Affairs and Ministry of Infrastructure and Environment, the Province of Fryslân, and the Northern Netherlands Provinces. The authors like to thank the participants of the research theme “Smart Water Grids” for the fruitful discussions and their financial support. The authors thank Brabant Water and Acquaint B.V. for providing the inspection data.

Appendix A. Supplementary material

Supplementary data to this article can be found online at https://doi.org/10.1016/j.engstruct.2020.110413.

References

[1] P.J.J.G. Geudens, J. van Grootveld, Dutch Drinking Water Statistics 2017, Den Haag, December 2017.
[2] V. Donazzolo, R. Yelf, Determination of wall thickness and condition of Asbestos Cement pipes in sewer rising mains using Surface Penetrating Radar, in: Proc. 13th Internarional Conf. Gr. Penetrating Radar, GPR 2010, 2010, pp. 1–5.
[3] Koo DH, Ariaratnam ST. Innovative method for assessment of underground sewer pipe condition. Autom. Constr. 2006;15(4):479–88.
[4] Smolders S, Verhoest L, De Gueldre G, Van De Steene B. Inspection of deteriorating asbestos cement force mains with georadar technique. Water Sci. Technol. 2009;60(4):995–1001.
[5] G. Robbins, D. Johnston, K. Laven, Predicting the remaining life of asbestos cement pipe with acoustic wall thickness testing, Pipelines 2014 From Undergr. to Forefr. Innov. Sustain. – Proc. Pipelines 2014 Conf., pp. 280–289, 2014.
[6] Bracken M, Johnston D, Coleman M. Asset management of asbestos cement pipes using acoustic methods: theory and case studies. Pipelines 2011;2011:225–35.
[7] Bracken M, Johnston D. Acoustic methods for determining remaining pipe wall thickness in asbestos cement and ferrous pipes. In: Pipelines 2009; 53(9);2009:271–281.
[8] Hu Y, Wang D, Chowdhury R. Condition assessment methods for AC pipe and current practices. Pipelines 2010 Climbing New Peaks to Infrastruct. Reliab. - Renew, Rehab, Reinvest – Proc. Pipelines 2010 Conf., 2010;386(306):867–877.
[9] Beuken R, Horst P, Diemel R, Mesman G. Mains condition assessment by echopulse, a validation of results. Procedia Eng 2014;89:1437–44.
[10] Zecchin AC, Gong J, Simpson AR, Lambert MF. Condition assessment in hydraulically noisy pipeline systems using a pressure wave splitting method. Procedia Eng 2014;89:1336–42.
[11] Gong J, Lambert M, Zecchin A, Simpson A, Arbon N, Il Kim Y. Field study on non-invasive and non-destructive condition assessment for asbestos cement pipelines by time-domain fluid transient analysis. Struct Heal Monit 2016;15(1):113–24.

[12] Zhang C, Gong J, Zecchin A, Lambert M, Simpson A. Faster inverse transient analysis with a head-based method of characteristics and a flexible computational grid for pipeline condition assessment. J Hydraul Eng 2018;144(4):1–12.
[13] Zhang C, Gong J, Lambert MF, Simpson AR, Zecchin AC. Sensor placement strategy for pipeline condition assessment using inverse transient analysis. Water Resour Manage 2019;33(8):2761–74.
[14] Zeng W, Gong J, Cazzolato BS, Zecchin AC, Lambert MF, Simpson AR. Condition assessment of pipelines using a Bi-directional layer-peeling method and a dual-sensor configuration. J Sound Vib 2019;457:181–96.
[15] El-Zahab S, Zayed T. Leak detection in water distribution networks: an introductory overview. Smart Water 2019;4(1).
[16] Grigg NS. Assessment and renewal of water distribution systems. J/Am Water Work Assoc 2005;97(2):58–68.
[17] Martini A, Troncossi M, Rivola A. Leak detection in water-filled small-diameter polyethylene pipes by means of acoustic emission measurements. Appl Sci 2017;7(1).
[18] Xie X, Hou D, Tang X, Zhang H. Leakage identification in water distribution networks with error tolerance capability. Water Resour Manage 2019;33(3):1233–47.
[19] Wong L, et al. Leak detection in water pipes using submersible optical optic-based pressure sensor. Sensors (Switzerland) 2018;18(12):1–17.
[20] Kayaalp F, Zengin A, Kara R, Zavrak S. Leakage detection and localization on water transportation pipelines: a multi-label classification approach. Neural Comput Appl 2017;28(10):2905–14.
[21] Cody R, Harmouche J, Narasimhan S. Leak detection in water distribution pipes using singular spectrum analysis. Urban Water J 2018;15(7):636–44.
[22] Roy U. Leak detection in pipe networks using hybrid ANN method. Water Conserv Sci Eng 2017;2(4):145–52.
[23] Ould Naffa S, Goueygou M, Piwakowski B, Buyle-Bodin F. Detection of chemical damage in concrete using ultrasound. Ultrasonics 2002;40(1–8):247–51.
[24] Demčenko A, Visser HA, Akkerman R. Ultrasonic measurements of undamaged concrete layer thickness in a deteriorated concrete structure. NDT E Int 2016;77:63–72.
[25] Hernandez Delgadillo H, Kern B, Loendersloot R, Yntema D, Akkerman R. A methodology based on pulse-velocity measurements to quantify the chemical degradation levels in thin mortar specimens. J Nondestruct Eval 2018;37(4).
[26] Delgadillo HH, Loendersloot R, Akkerman R, Yntema D. Development of an inline water mains inspection tech nology. IEEE Int Ultrason Symp IUS 2016.
[27] Wang D, Cullimore DR. Bacteriological challenges to asbestos cement water distribution pipelines. J Environ Sci 2010;22(8):1203–8.
[28] Wang D, Cullimore R, Hu Y, Chowdhury R. Biodeterioration of asbestos cement (AC) pipe in drinking water distribution systems. Int Biodeterior Biodegrad 2011;65(6):810–7.
[29] Bouchaala F, Payan C, Garnier V, Balayssac JP. Carbonation assessment in concrete by nonlinear ultrasound. Cem Concr Res 2011;41(5):557–9.
[30] Carde C, François R. Effect of the leaching of calcium hydroxide from cement paste on mechanical and physical properties. Cem Concr Res 1997;27(4):539–50.
[31] Wang D, Hu Y, Chowdhury R. Examination of asbestos cement pipe deterioration with scanning electron microscopy. In: Pipelines 2011 A Sound Conduit Shar. Solut. - Proc. Pipelines 2011 Conf., no. 306, pp. 65–78, 2011.
[32] Burlion N, Bernard D, Chen D. X-ray microtomography: application to microstructure analysis of a cementitious material during leaching process. Cem Concr Res 2006;36(2):346–57.
[33] Chowdhury R, Hu Y, Wang D. Condition evaluation of asbestos cement water mains. Pipelines 2012;2012(306):288–97.
[34] Stark G, Charlton R. Class 150 Asbestos Cement (AC) Watermain Pipe Condition Evaluation Deep Bay Water District 2008;106(December):3019–3032.